
Fourier-Mixed Window Attention: Accelerating Informer for Long Sequence Time-Series Forecasting

Nhat Thanh Tran¹ Jack Xin¹

Abstract

We study a fast local-global window-based attention method to accelerate Informer for long sequence time-series forecasting. While window attention being local is a considerable computational saving, it lacks the ability to capture global token information which is compensated by a subsequent Fourier transform block. Our method, named FWin, does not rely on query sparsity hypothesis and an empirical approximation underlying the ProbSparse attention of Informer. Through experiments on univariate and multivariate datasets, we show that FWin transformers improve the overall prediction accuracies of Informer while accelerating its inference speeds by 1.6 to 2 times. We also provide a mathematical definition of FWin attention, and prove that it is equivalent to the canonical full attention under the block diagonal invertibility (BDI) condition of the attention matrix. The BDI is shown experimentally to hold with high probability for typical benchmark datasets.

1. Introduction

Recent progress in long sequence time-series forecasting (LSTF) has been led by either transformers with sparse attention ((Zhou et al., 2021) and references therein) or attention in combination with signal pre-processing such as seasonal-trend decomposition (Zhou et al., 2022) or adopting auto-correlation to account for periodicity in the data (Wu et al., 2021). On the other hand, Fourier transform has been proposed as an alternative mixing tool in lieu of standard attention (Vaswani et al., 2017) to speed up prediction in natural language processing (NLP) tasks (FNet, (Lee-Thorp et al., 2021)). Though Fourier transform is meant to mimic the mixing functions of multi-

layer perceptron (MLP, (Tolstikhin et al., 2021)), it is not well-understood why it works and when assistance from attention layers remain necessary to maintain performance. In computer vision (CV), Fourier transform is also used as a filtering step in early stages of transformer (GFNet, (Rao et al., 2021)) to enhance a fully attention-based architecture. A recent advance in CV is to adopt window attention to reduce quadratic complexity of full attention (Vaswani et al., 2017). In shifted window attention (Swin (Liu et al., 2022)), the attention is first computed on non-overlapping windows as a local approximation, then on shifted window configurations to spread local attention globally in the image domain. This local-global approximation of full attention occurs entirely in the image domain, and is repeated over multiple stages in the network. The advantage is that the recipe is independent of the data distribution. In contrast, the ProbSparse self-attention of Informer (Zhou et al., 2021; 2023) relies on long tail data distribution to select the top few queries.

We are interested in developing an efficient window-based attention to replace ProbSparse attention and accelerate Informer with no prior knowledge of data properties such as periodicity (seasonality) so that our method is applicable in a general context of time series. We also refrain from pre-processing data to increase performance as this step can be added later. The main issue is how to globalize the local window attention without performing shifts, since Informer only has two attention blocks in the encoder and is unable to facilitate repeated window shifting as in a deeper network Swin (Liu et al., 2022).

We propose to replace ProbSparse attention of Informer via a (local) window attention followed by a Fourier transform (mixing) layer, a novel local-global attention which we call Fourier-Mixed window attention (FWin). The resulting network, FWin Transformer, aims to reduce the complexity of the full attention (Vaswani et al., 2017) and approximate its functionality by mixing the window attention. Instead of shifting windows for globalization (Liu et al., 2022), we employ the parameter free fast Fourier Transform (FFT) to generate connections among the tokens. The strategy allows the window attention layer to focus on learning local information, while the Fourier layer effectively mixes

^{*}Equal contribution ¹Department of Mathematics, University of California, Irvine, California, USA. Correspondence to: Nhat Thanh Tran <nhattt@uci.edu>.

Preliminary work. Under review by the International Conference on Machine Learning (ICML).

tokens and spreads information globally. In the ablation study, we find that the network prediction accuracy is lower if we replace ProbSparse by only Fourier mixing as in FNet (Lee-Thorp et al., 2021) without the help of window attention. Besides conducting extensive experiments on FWin to support our methodology, we also provide a mathematical formulation of mix window attention and prove that it is equivalent to the canonical attention.

Our main contributions in this paper are summarized below.

- We propose FWin and replace the ProbSparse self attention block (Fig. 1, left) via a window self-attention block followed by a Fourier mixing layer (Fig. 1, right) in both the encoder and decoder of Informer (Zhou et al., 2021; 2023).
- We show experimentally that FWin either increases or maintains Informer’s performance level while significantly accelerating its inference speed (by about 1.6 to 2 times) on both univariate and multivariate LSTF data. The training times of FWin are consistently lower than those of Informer across various data. Inference speeds of FWin exceed those of Fedformer (Zhou et al., 2022) and Autoformer (Wu et al., 2021) by a factor of 5 to 10 with shorter training times overall.
- We propose FWin-S, a light weight version of FWin, by removing Fourier mixing layer in the decoder (Fig. 1, right); and present its competitive performance with faster inference speed.
- We provide a mathematical formulation of mix window attention and prove that it is equivalent to the canonical attention under block diagonal invertibility (BDI) condition of the attention matrix.

Organization. This paper will proceed as follows: In section 2, we provide background on full attention, window attention, Fourier mixing. In Section 3, we present FWin methodology and its complexity. In section 4, we present experimental results and analysis. In section 5, we mathematically formulate mix window attention and prove it is equivalent to canonical attention. We show that FWin is a special case of mix window attention. The paper ends with concluding remarks. Related works, ablation studies, FWin in a nonlinear/non-parametric regression model, and more experimental details are provided in the Appendix.

2. Background and Preliminary

Canonical Full Attention Given an input sequence $x \in \mathbb{R}^{L \times d_{\text{model}}}$, where L is the sequence length and d_{model} is the

embedded dimension of the model. The input x is then converted into queries (Q), keys (K), values (V) as:

$$Q = xW_Q + b_Q, K = xW_K + b_K, V = xW_V + b_V,$$

where $W_Q, W_K, W_V \in \mathbb{R}^{d_{\text{model}} \times d_{\text{attn}}}$ are the weighted matrix, and $b_Q, b_K, b_V \in \mathbb{R}^{L \times d_{\text{attn}}}$ are the bias matrix. In most cases, we will have $d_{\text{model}} = d_{\text{attn}}$, thus we will refer to d_{model} for the remaining of the paper.

We have

$$\text{Attn}_f(Q, K, V) = \text{softmax}(QK^T / \sqrt{d_{\text{model}}})V, \quad (1)$$

where $\text{Attn}_f(\cdot)$ is the attention function.

We refer to the function in (1) as full attention (Vaswani et al., 2017), because it involves the interaction of all the key and query pairs. The final output is the weighted sum of all the values.

Window Attention The full attention computation involves the dot product between each query and all the keys. However, for tasks with large sequence lengths such as processing of high resolution images, the computational cost of full attention can be significant (Liu et al., 2022). As in Swin Transformer, we divide the sequence into subsequences of smaller length, compute sub-attention for each of the subsequences individually and then concatenate all the sub-attention together. Namely, we divide sequence x into N subsequences: $x^{(1)}, x^{(2)}, \dots, x^{(N)}$, such that $x = [x^{(1)}, x^{(2)}, \dots, x^{(N)}]^T$. Each $x^{(i)} \in \mathbb{R}^{L/N \times d_{\text{model}}}$ for $i = 1, 2, \dots, N$, where $N = L/w$, w is a fixed window size. This implies we divide the queries, keys and values as follow $Q = [Q^{(1)}, Q^{(2)}, \dots, Q^{(N)}]^T$, $K = [K^{(1)}, K^{(2)}, \dots, K^{(N)}]^T$, $V = [V^{(1)}, V^{(2)}, \dots, V^{(N)}]^T$. Thus we compute attention for each subsequence as follows:

$$\text{Attn}_f(Q^{(i)}, K^{(i)}, V^{(i)}) = \text{softmax}\left(\frac{Q^{(i)}K^{(i)T}}{\sqrt{d_{\text{model}}}}\right)V^{(i)}. \quad (2)$$

After computing the attention for each subsequence, we concatenate the sub attentions to form the window attention:

$$\text{Attn}_w(Q, K, V) = \begin{bmatrix} \text{Attn}_f(Q^{(1)}, K^{(1)}, V^{(1)}) \\ \vdots \\ \text{Attn}_f(Q^{(N)}, K^{(N)}, V^{(N)}) \end{bmatrix}. \quad (3)$$

In window attention, we compute attention on a window-by-window basis. Within each window, all the keys are multiplied with the corresponding query within that window. The output is the weighted sum of the values within the same window, rather than considering the entire set of values. This approach reduces the computational cost of computing attention on a sequence of length L from $\mathcal{O}(L^2)$ of full attention to $\mathcal{O}(Lw)$, where w is a fixed window size.

A natural question that arises is how well the window attention compares to full attention. If $\text{softmax}(QK^T/\sqrt{d_{\text{model}}})$ is almost diagonal, meaning that most of the entries apart from the diagonal are close to zero, then window attention can be considered a good approximation of full attention. However, this is often not the case as seen in a nonlinear regression model in the Appendix I.

Window attention restricts the interaction between queries and keys by only allowing queries to attend to their local window keys. As a result, window attention provides limited or local information. On the other hand, full attention enables queries to attend to keys that are further away, allowing for global interaction. If we replace full attention with window attention, our model may lack a comprehensive understanding of global information. Therefore, it is desirable for our model to retain some level of global information when using window attention as a substitute for full attention. To incorporate global information, Swin Transformer (Liu et al., 2022) introduces shifted window attention. In this approach, before dividing the input sequence x into sub-sequences, one performs a circular shift of the indices of x by certain value. This shift allows the ending values of x to become the starting values of our input. The circular shifting process is repeated for each consecutive window attention layers.

FNet Another way to promote global token interaction is by Fourier transform as proposed in FNet (Lee-Thorp et al., 2021). Given input $x \in \mathbb{R}^{L \times d_{\text{model}}}$, one computes Fourier transform along the model dimension (d_{model}), then along the time dimension (L), finally taking real part to arrive at:

$$y = \mathcal{R}(\mathcal{F}_{\text{time}}(\mathcal{F}_{\text{model}}(x))), \quad (4)$$

where \mathcal{F} is 1D discrete Fourier transform (DFT), and \mathcal{R} is the real part of a complex number. Since DFT is free of learning parameter, one would eventually pass the transformed sequence through a Feed Forward fully-connected layer (FC). This approach can be interpreted as the Fourier transform being an effective mechanism for mixing sub-sequences (tokens) (Lee-Thorp et al., 2021). By applying the Fourier transform, the Feed Forward layer gains access to all the tokens.

3. Methodology

Informer Overview The input $x \in \mathbb{R}^{L \times d_{\text{data}}}$ passes through an embedding layer to encode the time scale information and return $X \in \mathbb{R}^{L \times d_{\text{model}}}$. In the encoder, each layer consists of an attention block followed by a distilling convolution with MaxPool of stride 2 and a down-sampling to halve dimension. Thus, with 2 encoder layers, the time dimension of the first attention block is L , while the second block input is $L/2$. For both efficiency and causality, the decoder attention has a masked multi-head Prob-

Sparse self-attention structure, see Fig. 1 (left) for an overview. The ProbSparse self-attention (Zhou et al., 2021) relies on a sparse query measurement function (an analytical approximation of Kullback-Leibler divergence) so that each key attends to only a few top queries for computational savings. The sparse query hypothesis or equivalently the long tail distribution of self-attention feature map is based on softmax scores in self-attention of a 4-layer canonical transformer trained on ETTh1 data set (Appendix C, (Zhou et al., 2021)).

Our Approach We introduce Fourier mixed window attention (FWin) to the self-attention blocks in the encoder and decoder of Informer. Specifically, we replace the ProbSparse self-attention blocks in the encoder and decoder with window attention followed by a Fourier mixing layer. We also replace multi-head cross-attention in the decoder by a window multi-head cross-attention. Fig. 1 (right) illustrates the key components of FWin Transformer. *Different from ProbSparse attention, our FWin approach does not rely on whether the query sparse hypothesis holds on a data set.*

We remark that our model adopted a modified version of the FNet architecture where Fourier transform is applied to the input along the model and the time dimensions without a subsequent Feed Forward layer. Partly this is due to the Feed Forward layer already present in the decoder of Informer before the output (Fig. 1, left). We denote this specific component as **Fourier Mix** in our proposed FWin architecture, as depicted in Fig. 1, right frame. If the Fourier Mix is removed from the decoder, we have a lighter model called FWin-S, which turns out to be a competitive design as well (see section 4).

Motivation Our model aims to capture both the short and long variations in the sequential data. The high frequency part represents local fluctuation, while the low frequency part describes the overall trend of the data. To achieve this, we utilize a combination of window attention and Fourier transform.

The window attention mechanism limits interactions among tokens, enabling the attention layer to learn the local time fluctuations. To capture the overall trend, the tokens need to be mixed beyond the window boundaries. This is achieved by leveraging the Fourier transform.

Another interpretation of the Fourier Mix layer is that the Fourier transform in the encoder maps the time domain to the frequency domain. As a result, the cross attention layer in the decoder must operate on the frequency domain. To achieve this, the model applies the Fourier transform to the decoder’s input before passing it to the cross attention layer. Subsequently, the FC layer maps the output of the cross attention from frequency domain back to the time domain.

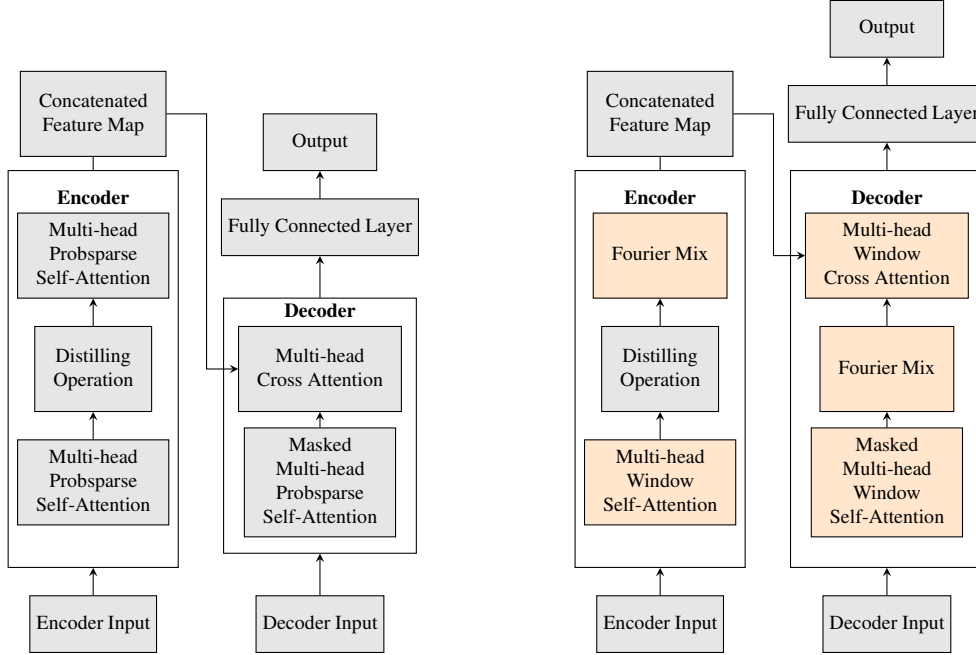


Figure 1. Model comparison: Informer (left), FWin (right, orange color denotes our contributions); FWin-S (FWin with its decoder’s Fourier Mix block removed).

By combining window attention (local) and Fourier transform (global), our model gains the ability to capture both the local time fluctuations and overall trend of the data. This comprehensive approach ensures that our model can effectively capture the complex dynamics present in the sequential data.

Encoder Each encoder layer is defined as either a window attention layer or a Fourier Mix layer. The layers are interwoven, with the first layer being a window attention. Subsequent layers are connected by a distillation operation. For example, a 3-layer encoder will consist of a window attention layer, a distillation operation, and a Fourier Mix layer, another distillation operation, and finally another window attention layer. Fig. 1 illustrates an encoder with 2 layers.

Decoder In the decoder, a layer composed of a masked window self-attention followed by a Fourier Mix and then window cross attention with layer normalization in between. Towards the end of the layer, convolutions and layer normalization are applied. Fig. 1 shows a decoder with one layer.

Window Cross Attention In a self-attention layer, the query and key vectors have the same time dimension, allowing us to use the same window size to split these vectors. However, in the case of cross attention, this may not hold true, especially if the encoder includes dimension reduction layers. In such cases, the key and value vectors may have a smaller time dimension compared to the query vec-

tors, which originate from the decoder. Additionally, the encoder and decoder inputs may have different input time dimensions, as is the case in our specific problem. To ensure equal number of attention windows in cross attention, we divide the query, key, and value vectors based on the number of windows rather than the window size. This adjustment accounts for varying time dimensions and guarantees a consistent number of attention windows for the cross attention operation.

Complexity With the replacements in the attention computation, our approach offers significant complexity reduction compared to Informer. In the encoder, the first attention layer partitions the time dimension of the input by a window of size w , by default $w = 24$, resulting in each window attention input having dimensions of $w \times d_{\text{model}}$. Thus the cost of this layer is $\mathcal{O}(Lwd_{\text{model}})$. Furthermore, in the second attention layer, the computation of attention is completely replaced by the Fourier Mix layer, eliminating three linear projections for query, key, and value vectors. Since we apply the FFT over the time dimension and the model dimension, the total cost for the Fourier Mix layer is $\mathcal{O}(Ld_{\text{model}} \log(Ld_{\text{model}}))$.

Tab. 1 is a summary of computational costs for each type of layers we discussed. Tab. 2 compares the complexities of Informer and FWin. The L^2d_{model} cost of Informer comes from full cross attention in its decoder (Fig. 1, left). In FWin, this cost is reduced to Lwd_{model} by window cross attention (Fig. 1, right).

Table 1. Computational complexities of major layers in Informer (Zhou et al., 2021) and FWin transformer.

Full Attention	$\mathcal{O}(L^2 d_{\text{model}})$
ProbSparse Attention	$\mathcal{O}(L \log(L) d_{\text{model}})$
Window Attention	$\mathcal{O}(L w d_{\text{model}})$
Fourier Mix	$\mathcal{O}(L d_{\text{model}} \log(L d_{\text{model}}))$

Table 2. Computational complexity comparison: Informer vs. FWin as shown in Fig. 1.

Informer	$\mathcal{O}(L \log(L) d_{\text{model}} + L \log(L) d_{\text{model}} + L \log(L) d_{\text{model}} + L^2 d_{\text{model}})$
FWin	$\mathcal{O}(L w d_{\text{model}} + L d_{\text{model}} \log(L d_{\text{model}}) + L w d_{\text{model}} + L d_{\text{model}} \log(L d_{\text{model}}) + L w d_{\text{model}})$

4. Experiment

Datasets We experiment on the following public benchmark datasets (additional ones are described in the Appendix E).

ETT (Electricity Transformer Temperature)¹: The dataset contains information of six power load features and target value “oil temperature”. We used two hour datasets ETTh₁ and ETTh₂, and the minute level dataset ETTm₁. The train/val/test split ratio is 6:2:2.

Weather (Local Climatological Data)²: The dataset contains local climatological data collected hourly in 1600 U.S. locations over 4 years from 2010 to 2013. The data consists of 11 climate features and target value “wet bulb”. The train/val/test split ratio is 7:1:2.

ECL (Electricity Consuming Load)³: This dataset contains electricity consumption (Kwh) of 321 clients. The data convert into hourly consumption of 2 year and “MT_320” is the target value. The train/val/test split ratio is 7:1:2.

Setup The default setup of the model parameters is shown in Tab. 3. For Informer, we used their up to date code at: <https://github.com/zhouhaoyi/Informer2020>, which incorporated all the functionalities described recently in (Zhou et al., 2023). In our experiments, we average over 5 runs. The total number of epochs is 6 with early stopping. We optimized the model with Adam optimizer, and the learning rate starts at $1e^{-4}$, decaying two times smaller every epoch. For fair comparison, all of the hyper-parameters are the same across all the models which were trained/tested on a desktop machine with four

¹<https://github.com/zhouhaoyi/ETDataset>

²<https://www.ncei.noaa.gov/data/local-climatological-data>

³<https://archive.ics.uci.edu/ml/datasets/ElectricityLoadDiagrams20112014>.

Table 3. Model default parameters.

d_{model}	512	Window size	24
d_{ff}	2048	Cross Attn Window no.	4
n_heads	8	Epoch	6
Dropout	0.05	Early Stopping Counter	3
Batch Size	32	Initial Lr	$1e^{-4}$
Enc.Layer no.	2	Dec.Layer no.	1

Nvidia GeForce 8G GPUs. Our source code is available upon request.

4.1. Results and Analysis

We present a summary of the univariate and multivariate evaluation results for all methods on 7 benchmark datasets in Tab. 4. MAE = $\frac{1}{n} \sum_{i=1}^n |y - \hat{y}|$ and MSE = $\frac{1}{n} \sum_{i=1}^n (y - \hat{y})^2$ are used as evaluation metrics. The best results are highlighted in boldface, and the total count at the bottom of the tables indicates how many times a particular method outperforms others per metric per dataset.

For univariate setting, each method produces predictions for a single output over the time series. From Tab. 4, we observe the following:

(1) FWin achieves the best performance with total count of 32.

(2) When comparing FWin and Informer, FWin outperforms the Informer by a margin of 50 to 16.

(3) FWin performs well on the ETT, Exchange, ILI datasets, it remains competitive for the Weather dataset. However, it performs worst on the ECL dataset. This could be due to the differences caused by the dataset, which is common in time-series model (Li et al., 2022), or Informer’s ProbSparse hypothesis satisfied well for this dataset.

(4) The average MSE reduction is 19.60%, and MAE is about 11.88%, when comparing FWin with Informer.

For the multivariate setting, each method produces predictions based on multiple features over the time series. From Tab. 4, we observe that:

(1) The light model FWin-S leads the count at 34 total, followed closely by FWin with a total count of 30.

(2) In a head to head comparison, FWin outperforms Informer by a large margin (59 to 7).

(3) FWin and FWin-S have close accuracies, yet FWin is overall better on both uni/multi-variate data-sets.

(4) The average MSE (MAE) reduction is about 16.33% (10.96%).

Optimizing the window size for each data set may increase

Table 4. Accuracy comparison on LSTF benchmark data (S/M denotes uni/multi-variate data), best results highlighted in bold.

Methods		Informer (S)		FWin (S)		FWin-S (S)		Informer (M)		FWin (M)		FWin-S (M)	
Metric		MSE	MAE	MSE	MAE	MSE	MAE	MSE	MAE	MSE	MAE	MSE	MAE
ETTh ₁	24	0.116	0.273	0.060	0.196	0.116	0.272	0.528	0.525	0.483	0.499	0.507	0.517
	48	0.170	0.333	0.102	0.257	0.141	0.302	0.764	0.665	0.638	0.592	0.695	0.626
	168	0.149	0.311	0.150	0.308	0.252	0.401	1.083	0.836	1.004	0.786	0.885	0.742
	336	0.160	0.323	0.108	0.261	0.397	0.519	1.270	0.920	1.094	0.821	1.022	0.814
	720	0.258	0.428	0.105	0.253	0.270	0.434	1.447	0.977	1.181	0.873	1.087	0.846
ETTh ₂	24	0.086	0.225	0.082	0.221	0.075	0.212	0.455	0.508	0.550	0.566	0.551	0.568
	48	0.164	0.318	0.125	0.277	0.140	0.299	2.368	1.241	0.774	0.664	0.792	0.680
	168	0.270	0.416	0.220	0.375	0.277	0.422	5.074	1.910	2.309	1.136	2.767	1.327
	336	0.324	0.458	0.244	0.396	0.277	0.425	3.116	1.460	2.461	1.187	2.663	1.337
	720	0.294	0.438	0.261	0.412	0.266	0.423	4.193	1.778	2.847	1.286	3.258	1.530
ETTh _m ₁	24	0.025	0.122	0.015	0.096	0.021	0.112	0.346	0.397	0.305	0.375	0.322	0.389
	48	0.055	0.181	0.031	0.132	0.032	0.135	0.480	0.482	0.408	0.444	0.436	0.467
	96	0.181	0.356	0.050	0.175	0.086	0.234	0.555	0.531	0.517	0.517	0.573	0.553
	288	0.279	0.450	0.179	0.341	0.173	0.334	0.943	0.746	0.831	0.688	0.794	0.691
	672	0.396	0.559	0.133	0.286	0.152	0.314	0.903	0.729	1.119	0.838	0.890	0.741
Weather	24	0.113	0.249	0.104	0.236	0.111	0.243	0.335	0.388	0.310	0.363	0.316	0.369
	48	0.196	0.332	0.172	0.315	0.176	0.310	0.395	0.434	0.379	0.419	0.379	0.415
	168	0.257	0.376	0.259	0.391	0.235	0.357	0.625	0.580	0.561	0.539	0.544	0.530
	336	0.275	0.397	0.338	0.458	0.262	0.388	0.665	0.611	0.630	0.585	0.598	0.574
	720	0.259	0.389	0.291	0.421	0.250	0.383	0.657	0.604	0.686	0.614	0.576	0.560
ECL	48	0.259	0.359	0.249	0.369	0.274	0.388	0.293	0.382	0.291	0.371	0.287	0.372
	168	0.332	0.410	0.408	0.479	0.403	0.472	0.292	0.386	0.302	0.379	0.295	0.378
	336	0.378	0.441	0.477	0.516	0.407	0.471	0.422	0.467	0.327	0.399	0.307	0.388
	720	0.373	0.444	0.568	0.577	0.376	0.455	0.600	0.559	0.344	0.408	0.311	0.390
	960	0.365	0.448	0.415	0.485	0.359	0.448	0.871	0.714	0.362	0.421	0.314	0.393
Exchange	96	0.305	0.435	0.294	0.409	0.281	0.414	0.991	0.797	0.828	0.733	0.762	0.694
	192	1.345	0.902	0.679	0.622	0.566	0.574	1.175	0.859	1.148	0.889	1.178	0.889
	336	2.441	1.253	0.949	0.761	0.785	0.703	1.581	0.999	1.301	0.960	1.344	0.971
	720	1.933	1.106	1.127	0.891	1.253	0.897	2.643	1.356	2.071	1.196	2.036	1.177
ILI	24	5.404	2.057	3.727	1.648	3.491	1.597	6.048	1.698	3.881	1.308	3.849	1.298
	36	4.384	1.849	3.124	1.534	3.023	1.528	5.871	1.681	4.036	1.331	4.024	1.316
	48	4.487	1.886	3.697	1.680	3.293	1.605	5.171	1.551	4.334	1.404	4.431	1.406
	60	5.179	2.035	4.141	1.788	3.767	1.734	5.273	1.553	4.547	1.443	4.600	1.438
Count		8		32		26		4		30		34	

Table 5. Post-fault voltage prediction accuracy comparison on power grid dataset (S/M same as in Tab. 4), best results highlighted in bold.

Methods	Informer		FWin		FWin-S		FEDformer		Autoformer		ETSformer		PatchTST		
Metric	MSE	MAE	MSE	MAE	MSE	MAE	MSE	MAE	MSE	MAE	MSE	MAE	MSE	MAE	
M	700	0.049	0.113	0.063	0.141	0.043	0.101	0.245	0.311	0.390	0.403	0.339	0.381	0.211	0.278
S	700	0.111	0.170	0.091	0.141	0.092	0.132	0.272	0.310	0.367	0.388	0.303	0.322	0.138	0.188

performance of our model. In Fig. 2, we present an ablation study of the effect of window sizes to the error for ETTh₁ on the long range metric of 720. In this case, a smaller window size, i.e. 6, would provide the best result. However, to keep the experiments consistent, we decide to keep the window size a fixed constant of 24. The time scale of a

dataset may impact the choice of window size. Many of the datasets have hourly time scale, thus choosing a window size of 24 is meaningful in covering a daily observation. Refer to Appendix C for full study of the effect of window sizes.

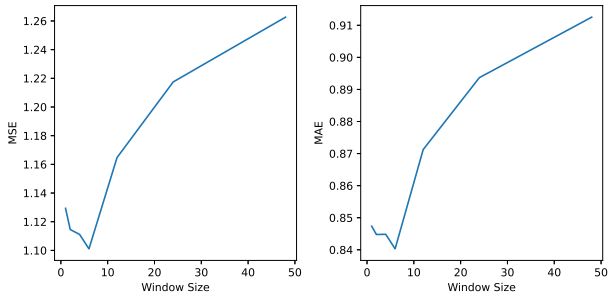


Figure 2. Window size versus error for ETTh1 multivariate data on the long range prediction metric of 720.

The experiments in the tables were conducted using similar hyper-parameters to those of Informer (Zhou et al., 2021) and Autoformer (Wu et al., 2021). Interestingly, FWin-S does so well without the Fourier Mix block in its decoder.

Informer’s prediction accuracies on the benchmark datasets in Tab. 4 have been largely improved by recent transformers such as PatchTST (Nie et al., 2023), Autoformer (Wu et al., 2021), FEDformer (Zhou et al., 2022) and ETSformer (Woo et al., 2022) designed with certain prior-knowledge of datasets, e.g. using auto-correlation or trend/seasonality decomposition. Like Informer, FWin has no prior-knowledge based operation, which helps to generalize better on non-stationary time series where seasonality is absent. Such a situation arises in post-fault decision making on a power grid where predicting transient trajectories is important for system operators to take appropriate actions (Li et al., 2020), e.g., a load shedding upon a voltage or frequency violation. We carry out experiments on a simulated New York/New England 16-generator 68-bus power system (Chow & Rogers, 2008; Zheng et al., 2022). The system has 88 lines linking the buses, and can be regarded as a graph with 68 nodes and 88 edges. The data set has over 2000 fault events, where each event has signals of 10 second duration. These signals contain voltage and frequency from every bus, and current from every line. The train/val/test split is 1000:350:750. Tab. 5 shows that FWin and FWin-S improve or maintain Informer’s accuracy in a robust fashion while the four recent transformers pale considerably in comparison. Fig. 3 illustrates model predictions on the power grid dataset (Chow & Rogers, 2008; Zheng et al., 2022). FWin and Informer outperform FEDformer, Autoformer, ETSformer, and PatchTST.

Besides performance, training and inference times of the models are our main concern and are summarized below:

(1) Compared to Informer, FWin achieves average speed up factors of **1.7** and **1.4** for inference and training times respectively. The ILI dataset has the lowest speed-up factor because both the input and the prediction lengths are small.

See Tab. 6 and Appendix C for breakdowns on six benchmark datasets, *similarly on other datasets in this paper*.

(2) FWin inference and training times are very close to those of FWin-S. This indicates that the Fourier Mix layer in the decoder adds a minimal overhead to the overall model. The FWin-S model exhibits the fastest inference and training times, as expected because it is the model with smallest parameter size here.

(3) FWin has approximately 8.1 million parameters, whereas Informer has around 11.3 million parameters under default settings, resulting in a reduction about 28%.

(4) The inference time for Informer increases with prediction length. FWin’s inference time exhibits minimal growth. The Exchange dataset demonstrates this effect as we used the same input length for all prediction lengths, and ran the models on a single GPU (see Appendix E.2).

Table 6. Average inference/training speed-up factors of FWin vs. Informer, see Appendix C for machine times.

Data	Feature	Inference	Train
ETTh ₁	Multivariate	1.66	1.34
ETTh ₁	Univariate	1.80	1.64
ETM ₁	Multivariate	1.70	1.30
ETM ₁	Univariate	1.68	1.34
Weather	Multivariate	1.70	1.28
Weather	Univariate	1.99	2.01
ECL	Multivariate	1.59	1.10
ECL	Univariate	2.01	1.53
Exchange	Multivariate	1.77	1.25
Exchange	Univariate	1.69	1.25
ILI	Multivariate	1.56	1.19
ILI	Univariate	1.62	1.29

5. Theoretical Results

Definition 5.1. Let $A \in \mathbb{R}^{L \times L}$ with a_{ij} its (i, j) -th entry. Let $w \in \mathbb{N}$ be a factor of L ; and for $\forall n \in \{1, \dots, L/w\}$, let A_n be the sub-matrix of A with entries $(a_{ij})_{i=nw, j=nw}^{i=(n-1)w+1, j=(n-1)w+1}$. We say A is block diagonally invertible (**BDI**) if for every n , A_n is invertible.

Definition 5.2. Let $Q, K \in \mathbb{R}^{L \times d}$ be the query, key matrix respectively. Define the attention matrix as:

$$\text{Attn}(Q, K) := \text{softmax}(QK^T / \sqrt{d}). \quad (5)$$

Definition 5.3. Let $Q, K, V \in \mathbb{R}^{L \times d}$ be the query, key, value matrix respectively. Define the full attention as:

$$\text{Attn}_f(Q, K, V) := \text{Attn}(Q, K)V. \quad (6)$$

Definition 5.4. Let $Q, K, V \in \mathbb{R}^{L \times d}$ be the query, key, value matrix respectively with q_i, k_i, v_i the i -th row of the

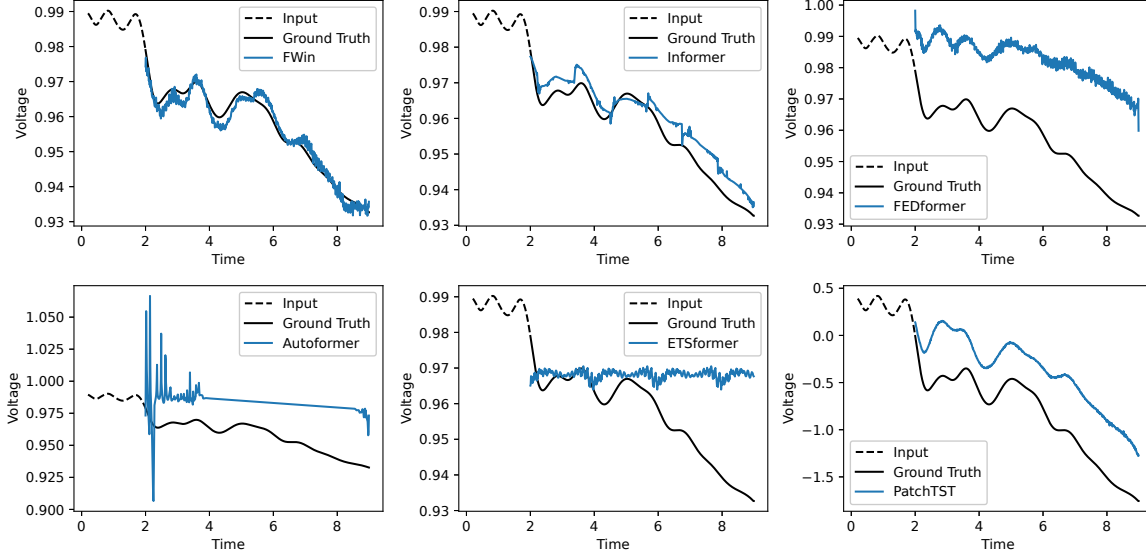


Figure 3. Univariate post fault prediction comparison (voltage vs. time in second) on power grid data (Chow & Rogers, 2008; Zheng et al., 2022): {FWin,Informer} outperform (FED,Auto,ETS)formers and PatchTST. The dashed line under 2 second duration is the input, to the right of which are the predictions vs. the ground truth (in black).

matrix Q, K, V . Let $w \in \mathbb{N}$ be the window size, such that w divides L . Define the window attention as:

$$\text{Attn}_w(Q, K, V, w) := \begin{bmatrix} \sum_{j \in J(1)} \frac{\exp(q_1 k_j^T v_j)}{\gamma_1} \\ \vdots \\ \sum_{j \in J(L)} \frac{\exp(q_L k_j^T v_j)}{\gamma_L} \end{bmatrix}. \quad (7)$$

Here $J(m) = \{Mw + 1, \dots, (M + 1)w\}$, where $M = \lfloor \frac{m-1}{w} \rfloor$; and

$$\gamma_m = \sum_{j \in J(m)} \exp(q_m k_j^T / \sqrt{d}). \quad (8)$$

Definition 5.5. Let $A \in \mathbb{R}^{L \times L}$ and Q, K, V, w be the same as in Definition 5.4, define the mixed window attention as:

$$\text{Attn}_{mw}(Q, K, V, w, A) := A \text{Attn}_w(Q, K, V, w) \quad (9)$$

Theorem 5.6. Let $Q, K, V \in \mathbb{R}^{L \times d}$. Let $w \in \mathbb{N}$ such that w divides L . If $\text{Attn}(Q, K)$ is BDI, then there exists a matrix $A \in \mathbb{R}^{L \times L}$ such that

$$\text{Attn}_f(Q, K, V) = \text{Attn}_{mw}(Q, K, V, w, A). \quad (10)$$

In particular, we can construct the exact value of A .

We provide the details of the proof in Appendix D.

Definition 5.7. Let $A \in \mathbb{R}^{L \times L}$ and Q, K, V, w be the same as defined in Definition 5.4, define the Fourier-mixed window attention as:

$$\text{Attn}_{Fwin}(Q, K, V, w, A) := A \mathcal{F}(\text{Attn}_w(Q, K, V, w)), \quad (11)$$

where \mathcal{F} is the discrete Fourier transform.

Corollary 5.8. Let Q, K, V and w be the same as defined in Theorem 5.6. If $\text{Attn}(Q, K)$ is BDI, then there exists a matrix $A \in \mathbb{C}^{L \times L}$ such that

$$\text{Attn}_f(Q, K, V) = \text{Attn}_{Fwin}(Q, K, V, w, A). \quad (12)$$

Definition 5.9. Let $A \in \mathbb{R}^{L \times L}$ and Q, K, V, w be the same as defined in Definition 5.4, define the Hartley-mixed window attention as:

$$\text{Attn}_{Hwin}(Q, K, V, w, A) := A \mathcal{H}(\text{Attn}_w(Q, K, V, w)), \quad (13)$$

where \mathcal{H} is the Hartley transform (Bracewell, 1986).

Corollary 5.10. Let Q, K, V and w be the same as defined in Theorem 5.6. If $\text{Attn}(Q, K)$ is BDI, then there exists a matrix $A \in \mathbb{R}^{L \times L}$ such that

$$\text{Attn}_f(Q, K, V) = \text{Attn}_{Hwin}(Q, K, V, w, A). \quad (14)$$

6. Conclusion

We introduced FWin Transformer and its light weight version FWin-S to successfully accelerate Informer by replacing its ProbSparse and full attention layers with window attention and Fourier mixing blocks in both encoder and decoder. The FWin attention approach does not rely on sparse attention hypothesis or periodic like patterns in the data. The experiments on univariate and multivariate datasets and theoretical guarantee demonstrated FWin's merit in fast inference on long sequence time-series forecasting while improving or maintaining Informer's performance.

In future work, we plan to further optimize and extend the FWin approach for accelerating transformers (including the prior-knowledge based ones) in various applications.

A. Related Work

Several types of attention models are related to our work here.

First, MLP mixers relax the graph similarity constraints of the self-attention and mix tokens with MLP projections. The original MLP-mixer (Tolstikhin et al., 2021) reaches similar accuracy as self-attention in vision tasks. However, such a method lacks scalability as a result of quadratic complexity of MLP projection, and suffers from parameter inefficiency for high resolution input.

Next, Fourier-based mixers apply Fourier transform to mix tokens in NLP and vision tasks. FNet (Lee-Thorp et al., 2021) resembles the MLP-mixer with token mixer being the classical discrete Fourier transform (DFT), without adaptive filtering on data distribution. Global filter networks (GFNs (Rao et al., 2021)) learn filters in the Fourier domain to perform depth-wise global convolution with no channel mixing involved. Also, GFN filters lack adaptivity that could negatively impact generalization. AFNO (Guibas et al., 2022) performs global convolution with dynamic filtering and channel mixing for better expressiveness and generalization. However, AFNO network parameter sizes tend to be much larger than those of the light weight vision transformer (ViT) models such as GFN-T (Rao et al., 2021), shift-window mixer Swin-T (Liu et al., 2022) and hybrid convolution-attention models MOAT-T (Yang et al., 2022), and mobile ViT (Mehta & Rastegari, 2022).

For long sequence time series forecasting, the Informer (Zhou et al., 2021; 2023) has a hybrid convolution-attention design with a probabilistic sparsity promoting function (ProbSparse) to reduce complexity of the standard self-attention and cross-attention. We shall adopt Informer as our baseline in this work, as it compares favorably vs. efficient transformers in recent years (see Tab. 1 and Tab. 2 in (Zhou et al., 2021)). More recent improvements on benchmark data sets include Autoformer (Wu et al., 2021), FEDformer (Zhou et al., 2022) and ETSformer (Woo et al., 2022), which are designed with certain prior-knowledge of datasets, e.g. using trend/seasonality decomposition and auto-correlation functions. However, they are not as robust on non-stationary time series as Informer (Tab. 5). Informer’s prediction is seen to generate spurious peaks on power grid data (3rd frame of Fig. 4), while FWin predictions appear smoother and free from such distortions. Comparing Informer with full Informer in the bottom frame of Fig. 4, we see that the cause of these distortions may be attributed to probsparse. Glassoformer (Zheng et al., 2022) uses group lasso penalty to enforce query sparsity and reduce complexity of full attention to speed up inference. Though this method works well on power grid data, its training time is higher than Informer since full attention

Table 7. Inference/training time comparison in seconds on LSTF benchmark data (S/M denotes uni/multivariate data, Inf denotes inference time).

Methods		Informer (S)		FWin (S)		FWin-S (S)		Informer (M)		FWin (M)		FWinS (M)	
Metric		Inf	Train	Inf	Train	Inf	Train	Inf	Train	Inf	Train	Inf	Train
ETTh1	24	0.280*	803.48*	0.112	267.6	0.107	262.0	0.153	75.9	0.100	50.8	0.094	49.1
	48	0.269	687.4	0.172	528.9	0.168	512.3	0.156	101.7	0.102	73.3	0.099	71.1
	168	0.297	718.4	0.180	548.3	0.176	537.9	0.175	205.5	0.106	156.4	0.101	147.7
	336	0.279	706.7	0.179	545.0	0.165	534.6	0.207	253.5	0.110	195.8	0.106	184.2
	720	0.303	671.4	0.176	516.0	0.171	504.9	0.321	676.8	0.179	557.4	0.176	554.7
ETTm1	24	0.153	381.4	0.102	281.3	0.098	263.5	0.193	1567.2	0.108	1029.7	0.102	1000.5
	48	0.155	411.7	0.099	310.6	0.096	292.4	0.158	417.8	0.116	317.7	0.095	296.4
	168	0.198	1476.0	0.108	1065.4	0.104	1027.3	0.200	1501.6	0.112	1102.6	0.104	1047.3
	288	0.278	2882.8	0.171	2203.9	0.166	2161.5	0.312	3046.3	0.184	2690.9	0.165	2304.4
	672	0.336	3058.9	0.178	2284.1	0.176	2259.0	0.368	3206.6	0.196	2761.3	0.176	2484.3
Weather	24	0.280*	2230.9*	0.111	734.8	0.106	729.6	0.228	623.4	0.142	474.9	0.136	453.9
	48	0.277*	2468.9*	0.114	753.7	0.110	741.8	0.170	318.2	0.101	237.0	0.097	229.9
	168	0.233	844.3	0.153	676.2	0.144	632.5	0.257	1084.2	0.153	819.1	0.151	790.7
	336	0.389	2558.2	0.241	2214.5	0.236	2098.3	0.419	2668.3	0.248	2257.2	0.229	2214.0
	720	0.476	2756.2	0.257	2399.0	0.243	2193.8	0.554	2911.3	0.283	2380.6	0.279	2331.9
ECL	48	0.276*	1354.2*	0.109	558.9	0.107	554.5	0.165	324.3	0.125	290.8	0.100	243.3
	168	0.218	925.8	0.117	626.3	0.113	618.1	0.202	811.1	0.121	696.6	0.112	624.0
	336	0.217	785.7	0.114	587.1	0.111	565.0	0.225	1462.3	0.138	1297.5	0.130	1167.9
	720	0.315	1337.8	0.180	1128.3	0.175	1117.7	0.371	3400.7	0.227	3352.1	0.220	3101.7
	960	0.417	1445.3	0.205	1171.8	0.199	1121.4	0.415	3703.0	0.246	3445.8	0.235	3398.6
Exchange	96	0.161	65.2	0.099	49.3	0.097	47.9	0.158	65.7	0.100	51.0	0.098	49.6
	192	0.164	79.7	0.102	62.6	0.099	59.9	0.164	81.9	0.103	64.4	0.100	61.5
	336	0.178	98.0	0.111	80.1	0.103	76.2	0.177	101.2	0.108	82.0	0.102	79.1
	720	0.226	145.4	0.118	121.2	0.115	114.7	0.271	149.1	0.120	124.1	0.114	117.8
ILL	24	0.155	7.9	0.099	5.8	0.097	5.5	0.152	9.4	0.097	7.0	0.094	6.9
	36	0.153	7.8	0.100	5.8	0.096	5.5	0.156	9.0	0.099	8.7	0.093	7.0
	48	0.150	7.4	0.097	6.0	0.097	5.7	0.155	9.1	0.100	7.3	0.096	7.3
	60	0.181	9.3	0.099	7.6	0.097	6.7	0.152	9.0	0.099	8.0	0.096	7.3

* using multiple GPUs compared to results by FWin/FWin-S on single GPU.

is involved in network training.

Table 8. FWin vs. FNet (Lee-Thorp et al., 2021) (replacing Prob-Sparse attention of Informer by Fourier-Mix followed by an FC layer) on multivariate ETTh1 data.

Model	FNet		FWin	
	MSE	MAE	MSE	MAE
24	0.490	0.502	0.483	0.499
48	0.562	0.543	0.638	0.592
168	1.052	0.806	1.004	0.786
336	1.194	0.869	1.094	0.821
720	1.349	0.948	1.181	0.873
Count	2		8	

Table 9. FWin vs. Swin (Liu et al., 2022) (replacing Fourier Mix in FWin by a shifted window attention) on multivariate ETTh1 data.

Model	Swin		FWin	
	MSE	MAE	MSE	MAE
24	0.567	0.540	0.483	0.499
48	0.685	0.627	0.638	0.592
168	1.016	0.810	1.004	0.786
336	1.161	0.877	1.094	0.821
720	1.095	0.844	1.181	0.873
Count	2		8	

B. Ablation Study

We examined the benefits of combining window attention and Fourier mixing by experiments on the ETTh1 dataset. Tab. 8 shows that Fourier-mixed window attention outper-

Table 10. Model accuracy comparison on traffic forecasting (S/M denotes univariate/multivariate data), best results highlighted in bold. The relative MSE difference between Informer and FWin on S/M is 5% /12.23%. The relative MAE difference between Informer and FWin on S/M data is 5.89% /11.68%.

Methods		Informer (S)		FWin (S)		FWin-S (S)		Informer (M)		FWin (M)		FWinS (M)	
Metric		MSE	MAE	MSE	MAE	MSE	MAE	MSE	MAE	MSE	MAE	MSE	MAE
Traffic	96	0.192	0.284	0.199	0.294	0.238	0.315	0.722	0.395	0.660	0.367	0.676	0.375
	192	0.212	0.301	0.218	0.315	0.245	0.322	0.779	0.422	0.672	0.368	0.693	0.382
	336	0.223	0.310	0.223	0.321	0.246	0.328	0.771	0.423	0.699	0.383	0.715	0.392
	720	0.246	0.334	0.266	0.364	0.340	0.410	0.892	0.484	0.761	0.414	0.704	0.383

forms using Fourier mixing alone (FNet (Lee-Thorp et al., 2021)) in accuracy. Tab. 9 suggests that Fourier-mixed window attention is better overall than shifted window attentions in the encoder. In view of Tab. 4, FWinS is better than Swin on metric 720 in MSE (comparable in MAE).

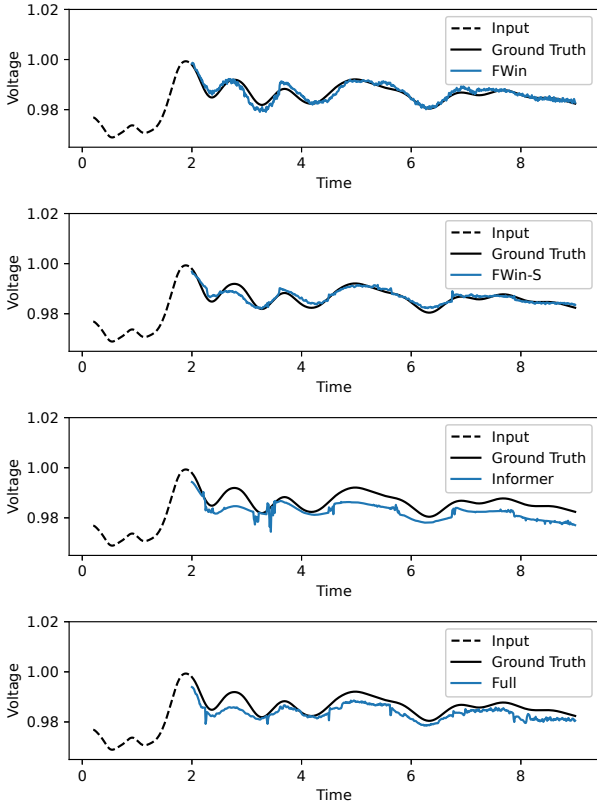


Figure 4. Univariate post fault prediction (voltage vs. time in second) on power grid data (Chow & Rogers, 2008; Zheng et al., 2022). FWin, FWin-S have “smooth” predictions while Informer has spurious jumps. Full in the bottom frame refers to Informer using full attention instead of probsparse. The dashed line to the left of 2 second is the input, to the right of which are the model predictions vs. the ground truth (in black).

C. Effect of window size parameter

Window size is an important parameter for FWin. In this section we will explore the effect of window size to model performance across many datasets presented in the paper. We present the results in Tab. 11. We observe that across the datasets, window size of 6 provides the best results overall. Window size of 1 provides competitive results compare to the best window size of 6. In general, under various window sizes, the performance is consistent.

D. Theoretical Results

Definition D.1. Let $A \in \mathbb{R}^{L \times L}$, with the (i, j) -th entry of A denoted by a_{ij} . Let $w \in \mathbb{N}$ be a factor of L . For every $n \in \{1, \dots, L/w\}$, let A_n be the sub-matrix of A such that the entries of A_n are composed of $(a_{ij})_{i=nw, j=nw}^{i=w(n-1)+1, j=w(n-1)+1}$. We say A is block diagonally invertible (BDI) if for every n , A_n is invertible.

Definition D.2. Let $Q, K \in \mathbb{R}^{L \times d}$ be the query, key matrix respectively. Define the attention matrix as:

$$\text{Attn}(Q, K) := \text{softmax}(QK^T/\sqrt{d}). \quad (15)$$

Definition D.3. Let $Q, K, V \in \mathbb{R}^{L \times d}$ be the query, key matrix respectively. Define the full attention as:

$$\text{Attn}_f(Q, K, V) := \text{softmax}(QK^T/\sqrt{d})V = \text{Attn}(Q, K)V. \quad (16)$$

Definition D.4. Let $Q, K, V \in \mathbb{R}^{L \times d}$ be the query, key, value matrix respectively with q_i, k_i, v_i the i -th row of the matrix Q, K, V . Let $w \in \mathbb{N}$ be the window size, such that w divides L . Define the window attention as:

$$\text{Attn}_w(Q, K, V, w) := \begin{bmatrix} \sum_{j \in J(1)} \frac{\exp(q_1 k_j^T / \sqrt{d}) v_j}{\gamma_1} \\ \vdots \\ \sum_{j \in J(L)} \frac{\exp(q_L k_j^T / \sqrt{d}) v_j}{\gamma_L} \end{bmatrix}. \quad (17)$$

Here $J(m) = \{Mw + 1, \dots, (M + 1)w\}$, where $M = \lfloor \frac{m-1}{w} \rfloor$. And

$$\gamma_m = \sum_{j \in J(m)} \exp(q_m k_j^T / \sqrt{d}). \quad (18)$$

Table 11. Accuracy comparison of FWin model using different window sizes for various dataset on the multivariate task. Best results highlighted in bold.

Window Size		1		2		4		6		12		24	
Metric		MSE	MAE	MSE	MAE	MSE	MAE	MSE	MAE	MSE	MAE	MSE	MAE
ETTh1	24	0.468	0.486	0.474	0.490	0.481	0.498	0.464	0.484	0.489	0.505	0.506	0.515
	48	0.599	0.565	0.606	0.571	0.611	0.580	0.592	0.569	0.575	0.554	0.586	0.561
	168	0.915	0.741	0.930	0.748	0.917	0.752	0.903	0.737	0.904	0.741	1.076	0.822
	336	1.049	0.782	1.002	0.769	1.000	0.774	0.978	0.766	0.998	0.772	1.070	0.813
	720	1.096	0.837	1.090	0.840	1.082	0.834	1.107	0.844	1.133	0.859	1.205	0.884
Weather	24	0.310	0.361	0.310	0.365	0.311	0.364	0.308	0.361	0.308	0.362	0.309	0.362
	48	0.382	0.419	0.380	0.421	0.378	0.420	0.380	0.420	0.381	0.421	0.381	0.421
	168	0.561	0.542	0.561	0.542	0.570	0.547	0.558	0.539	0.550	0.535	0.561	0.539
	336	0.631	0.592	0.626	0.586	0.610	0.577	0.629	0.587	0.612	0.578	0.618	0.580
	720	0.738	0.695	0.798	0.723	0.793	0.717	0.714	0.683	0.775	0.717	0.806	0.729
Exchange	96	1.195	0.910	1.066	0.869	1.297	0.951	1.261	0.941	1.132	0.891	1.136	0.886
	192	1.314	0.964	1.244	0.941	1.340	0.970	1.270	0.940	1.389	0.992	1.302	0.962
	336	1.916	1.134	2.034	1.166	1.944	1.137	1.885	1.128	2.225	1.225	2.055	1.176
	720	1.916	1.134	2.034	1.166	1.944	1.137	1.885	1.128	2.225	1.225	2.055	1.176
	Count	1		3		5		14		4		0	

Definition D.5. Let $A \in \mathbb{R}^{L \times L}$ and $Q, K, V, q_i, k_i, v_i, w$ be the same as defined in **Definition D.4**, define the mixed window attention as:

$$\text{Attn}_{mw}(Q, K, V, w, A) := A \text{Attn}_w(Q, K, V, w) \quad (19)$$

Theorem D.6. Let $Q, K, V \in \mathbb{R}^{L \times d}$. Let $w \in \mathbb{N}$ such that w divides L . If $\text{Attn}(Q, K)$ is BDI, then there exists a matrix $A \in \mathbb{R}^{L \times L}$ such that

$$\text{Attn}_f(Q, K, V) = \text{Attn}_{mw}(Q, K, V, w, A). \quad (20)$$

In particular, we can construct the exact value of A .

Proof. We have the i -th row of full attention is

$$\text{Attn}_f^i = \sum_{j=1}^L \frac{\exp(q_i^T k_j / \sqrt{d}) v_j}{\beta_i}, \quad (21)$$

where $\beta_i = \sum_{j=1}^L \exp(q_i^T k_j / \sqrt{d})$. Let α_{im} be the i, m entry of A , the i -th row of mixed window attention is

$$\text{Attn}_{mw}^i = \sum_{m=1}^L \alpha_{im} \sum_{j=Mw+1}^{(M+1)w} \frac{\exp(q_m^T k_j / \sqrt{d}) v_j}{\gamma_m}, \quad (22)$$

where $\gamma_m = \sum_{j \in J(m)} \exp(q_m^T k_j / \sqrt{d})$, with $J(m) = \{Mw+1, \dots, (M+1)w\}$, where $M = \lfloor \frac{m-1}{w} \rfloor$.

Consider the following cases:

- If $i = m$ and $j \in \{Mw+1, \dots, (M+1)w\}$, set $\frac{1}{\beta_i} = \frac{\alpha_{ii}}{\gamma_m}$.

- If $i \neq m$ and $j \in \{Mw+1, \dots, (M+1)w\}$ and $j \in \{Iw+1, \dots, (I+1)w\}$, where $I = \lfloor \frac{i-1}{w} \rfloor$, set $\alpha_{im} = 0$.

- If $i \neq m$ and $j \in \{Mw+1, \dots, (M+1)w\}$ and $j \notin \{Iw+1, \dots, (I+1)w\}$, where $I = \lfloor \frac{i-1}{w} \rfloor$. For each j we set

$$\frac{\exp(q_i k_j^T / \sqrt{d})}{\beta_i} = \sum_{m \in J(j)} \frac{\alpha_{im} \exp(q_m k_j^T / \sqrt{d})}{\gamma_m}. \quad (23)$$

For each i and set of $\{m, j\}$ pairs, we have to solve a system of w equations and unknowns. We now invoke the BDI assumption of $\text{Attn}(Q, K)$ to show that this system of equations has unique solution. Let C be the coefficient matrix of the right hand side of the system of equations in (23). We observe that C^T is invertible, because each row of C^T is a scaled version of a square sub matrix along the diagonal of $\text{Attn}(Q, K)$, and each square sub-matrix along the diagonal of $\text{Attn}(Q, K)$ is invertible. The invertibility of C then follows from that of C^T .

We completed the construction of A as claimed in the theorem. \square

Remark The BDI assumption in **Theorem D.6** is a sufficient condition and not a necessary condition. We only need BDI to solve the system of equations in Eq. 23. Equation 23 may be solvable even if BDI is not met. In this case, the solution will not be unique. In section H, we will show

in practice that BDI is satisfied by most of the datasets presented in this paper.

Definition D.7. Let $A \in \mathbb{R}^{L \times L}$ and Q, K, V, w be the same as defined in **Definition D.4**, define the Fourier-mixed window attention as:

$$\text{Attn}_{Fwin}(Q, K, V, w, A) := A\mathcal{F}(\text{Attn}_w(Q, K, V, w)), \quad (24)$$

where \mathcal{F} is the discrete Fourier transform.

Corollary D.8. Let Q, K, V and w be the same as defined in **Theorem D.6**. If $\text{Attn}(Q, K)$ is BDI, then there exists a matrix $A \in \mathbb{C}^{L \times L}$ such that

$$\text{Attn}_f(Q, K, V) = \text{Attn}_{Fwin}(Q, K, V, w, A). \quad (25)$$

Proof. From **Theorem D.6**, there exists $B \in \mathbb{R}^{L \times L}$ such that

$$\text{Attn}_f(Q, K, V) = \text{Attn}_{mw}(Q, K, V, w, B). \quad (26)$$

Thus if we let $A = BF^{-1}$, then we are done. \square

Definition D.9. Let $A \in \mathbb{R}^{L \times L}$ and Q, K, V, w be the same as defined in **Definition D.4**, define the Hartley-mixed window attention as:

$$\text{Attn}_{Hwin}(Q, K, V, w, A) := A\mathcal{H}(\text{Attn}_w(Q, K, V, w)), \quad (27)$$

where \mathcal{H} is the Hartley transform (Bracewell, 1986).

Corollary D.10. Let Q, K, V and w be the same as defined in **Theorem D.6**. If $\text{Attn}(Q, K)$ is BDI, then there exists a matrix $A \in \mathbb{R}^{L \times L}$ such that

$$\text{Attn}_f(Q, K, V) = \text{Attn}_{Hwin}(Q, K, V, w, A). \quad (28)$$

Proof. From **Theorem D.6**, there exists $B \in \mathbb{R}^{L \times L}$ such that

$$\text{Attn}_f(Q, K, V) = \text{Attn}_{mw}(Q, K, V, w, B). \quad (29)$$

Thus if we let $A = BH^{-1}$, then we are done. \square

E. Additional Experimental Data and Details

Exchange⁴ (Lai et al., 2018): The dataset contains daily exchange rates of eight different countries from 1990 to 2016. The train/val/test split ratio is 7:1:2.

ILI⁵: The dataset contains weekly recorded influenza-like illness (ILI) patients data from Centers for Disease Control and Prevention of the United States from 2002 to 2021. This describes the ratio of patients seen with ILI and the

total number of the patients. The train/val/test split ratio is 7:1:2.

Traffic⁶: The dataset contains hourly data from California Department of Transportation, describing the road occupancy rates measured by different sensors on San Francisco Bay area freeways. The train/val/test split ratio is 7:1:2. Results on the traffic data are in Tab. 10 where FWin are comparable to (much better than) Informer on univariate (multivariate) data. The relative MSE difference between Informer and FWin on univariate (multivariate) data is 5% (12.23%). The relative MAE difference between Informer and FWin on univariate (multivariate) data is 5.89% (11.68%).

E.1. Setup of experiments

For all the experiments to compute the errors, the encoder’s input sequence and the decoder’s start token are chosen from $\{24, 48, 96, 168, 336, 720\}$ for the ETTh₁, ETTh₂, Weather and ECL dataset, and from $\{24, 48, 96, 192, 288, 672\}$ for the ETTm dataset. The default window size is 24. We use a window size of 12 when the encoder’s input sequence is 24. For the Exchange, ILI, and Traffic datasets, we use the same hyper-parameters as those provided in Autoformer. The encoder’s input sequence is 96 and decoder’s input sequence is 48. The window size is 24 for Exchange and Traffic. For ILI, we use an input length of 36 for the encoder and 18 for decoder, with window size of 6. The number of windows on the cross attention is set to 3. The models are trained for 6 epochs with learning rate adjusted by a factor of 0.5 every epoch.

For the power grid dataset (Chow & Rogers, 2008; Zheng et al., 2022), the encoder and decoder inputs are set to 200. The prediction length is 700, and the window size is 25. The models are trained for 80 epochs with an early stopping counter of 30. The learning rate is adjusted every 10 epochs by a factor of 0.85.

E.2. Setup of train/inference time

The results in Tab. 7 are obtained by conducting experiments using the same set of hyper-parameters for each model and dataset. The inference time represents the total duration taken by a model to generate 30 predictions. The training time is a run of simulation each consisting of 6 epochs. Run time is very sensitive to machine conditions, thus we ran all of the simulations using the same machine, under the same traffic conditions.

⁶<https://pems.dot.ca.gov>

⁴<https://github.com/laiquokun/multivariate-time-series-data>

⁵<https://gis.cdc.gov/grasp/fluview/fluportaldashboard.html>

Table 12. Standard deviation comparison on LSTF benchmarks (S/M for uni/multivariate), best results highlighted in bold.

Methods		FWin (S)		Informer (S)		FWin (M)		Informer (M)	
Metric		MSE	MAE	MSE	MAE	MSE	MAE	MSE	MAE
ETTh ₁	24	0.012	0.019	0.022	0.029	0.011	0.008	0.058	0.039
	48	0.019	0.027	0.036	0.043	0.043	0.028	0.115	0.069
	168	0.030	0.035	0.062	0.063	0.061	0.030	0.047	0.029
	336	0.012	0.016	0.057	0.057	0.033	0.013	0.142	0.063
	720	0.014	0.015	0.051	0.055	0.055	0.019	0.048	0.017
ETTh ₂	24	0.005	0.008	0.004	0.006	0.043	0.026	0.028	0.021
	48	0.010	0.011	0.015	0.016	0.140	0.068	0.239	0.059
	168	0.028	0.024	0.018	0.015	0.108	0.023	0.555	0.108
	336	0.022	0.019	0.036	0.025	0.169	0.044	0.407	0.111
	720	0.008	0.007	0.019	0.013	0.162	0.033	0.292	0.050
ETTm ₁	24	0.002	0.009	0.009	0.025	0.012	0.007	0.045	0.032
	48	0.006	0.013	0.020	0.042	0.021	0.010	0.037	0.025
	96	0.016	0.023	0.040	0.051	0.060	0.031	0.054	0.040
	288	0.019	0.018	0.066	0.054	0.043	0.017	0.136	0.070
	672	0.033	0.039	0.083	0.069	0.102	0.043	0.058	0.028
Weather	24	0.006	0.008	0.004	0.012	0.010	0.011	0.003	0.001
	48	0.010	0.014	0.008	0.009	0.003	0.001	0.005	0.003
	168	0.010	0.013	0.005	0.005	0.011	0.006	0.006	0.014
	336	0.035	0.029	0.011	0.011	0.012	0.007	0.015	0.007
	720	0.011	0.009	0.025	0.010	0.015	0.012	0.011	0.007
ECL	48	0.011	0.010	0.015	0.011	0.011	0.010	0.011	0.007
	168	0.006	0.005	0.017	0.009	0.006	0.004	0.003	0.004
	336	0.030	0.018	0.007	0.009	0.004	0.003	0.046	0.026
	720	0.047	0.021	0.032	0.021	0.007	0.007	0.090	0.043
	960	0.034	0.018	0.100	0.054	0.008	0.006	0.088	0.044
Exchange	96	0.071	0.035	0.068	0.039	0.115	0.045	0.130	0.046
	192	0.188	0.060	0.278	0.083	0.155	0.052	0.024	0.009
	336	0.162	0.063	0.138	0.032	0.065	0.029	0.053	0.016
	720	0.227	0.078	0.175	0.048	0.119	0.041	0.199	0.051
ILI	24	0.126	0.035	0.211	0.046	0.137	0.031	0.142	0.032
	36	0.124	0.037	0.077	0.015	0.022	0.014	0.180	0.039
	48	0.148	0.037	0.057	0.017	0.044	0.011	0.168	0.031
	60	0.082	0.019	0.147	0.027	0.036	0.014	0.192	0.036
Count		42		23		43		26	

F. FWin Accuracy with Standard Deviation

In Tab. 12, we include the standard deviations of the FWin and Informer accuracies shown in the paper. The standard deviations are computed using five experimental runs.

G. Inference and Training Time Comparison with Auto/Fed/ETSformers

We compare inference and training times of FWin transformer with those of Autoformer (Wu et al., 2021), FED-former (Zhou et al., 2022) and ETSformer (Woo et al., 2022) in Tab. 13 and Tab. 14. These three transformers

are designed to improve accuracies of Informer with prior-knowledge of datasets. e.g. using trend/seasonality decomposition. In contrast, FWin has no prior-knowledge based operation, exactly the same as Informer. We use the default set of hyper-parameters provided in their respective papers. The inference time represents the total duration taken by a model to generate 30 predictions. The training time is a run of simulation each consisting of 6 epochs.

H. Condition Number of Attention Matrix

Theorem 5.6 requires the attention matrix to be BDI. In this section, we will verify that in practice BDI is satisfied by

Table 13. Inference/training times (seconds) vs. prior-knowledge dependent (noted by *) transformers on univariate datasets.

Methods		Autoformer*		FEDformer*		ETSformer*		FWin	
Metric		Inference	Train	Inference	Train	Inference	Train	Inference	Train
ETTh ₁	24	0.7056	242.70	0.7039	379.09	0.1766	113.76	0.1123	267.57
	48	0.6717	276.59	0.7530	431.62	0.1987	191.99	0.1720	528.90
	168	0.8726	365.88	0.7715	548.20	0.1972	351.06	0.1804	548.34
	336	0.9025	526.16	0.7582	695.77	0.3041	736.35	0.1794	545.03
	720	1.0161	860.87	0.7857	971.53	0.2889	677.74	0.1760	516.01
ETTm ₁	24	0.6795	924.45	0.6956	1421.72	0.1782	561.69	0.1015	281.33
	48	0.6926	1024.84	0.6699	1632.67	0.1770	580.23	0.0991	310.58
	168	0.7326	1119.16	0.8113	2133.04	0.1786	593.16	0.1076	1065.35
	288	0.9187	1981.56	0.8088	2546.94	0.1832	803.27	0.1714	2203.90
	672	1.0137	3659.89	0.8631	3963.63	0.1870	1163.27	0.1776	2284.08
ECL	48	0.6846	477.14	0.7202	890.71	0.2191	824.47	0.1091	558.92
	168	0.8439	641.90	0.7641	1163.12	0.2142	908.73	0.1171	626.27
	336	0.8577	956.78	0.7767	1404.01	0.2180	941.34	0.1143	587.11
	720	1.0372	1654.55	0.7695	2067.92	0.2732	1048.18	0.1804	1128.26
	960	1.2184	2548.90	0.7963	2419.27	0.2949	1058.18	0.2054	1171.78

Table 14. Inference/training times (seconds) vs. prior-knowledge dependent (noted by *) transformers on multivariate datasets.

Methods		Autoformer*		FEDformer*		ETSformer*		FWin	
Metric		Inference	Train	Inference	Train	Inference	Train	Inference	Train
ETTh ₁	24	0.6884	220.29	0.6706	359.67	0.1758	122.99	0.0996	50.83
	48	0.7778	248.73	0.7083	413.29	0.1749	190.34	0.1018	73.34
	168	0.9023	369.76	0.8082	565.03	0.2009	329.34	0.1059	156.38
	336	0.8885	530.38	0.7562	711.03	0.2752	702.21	0.1098	195.80
	720	1.0892	866.92	0.7403	997.00	0.2854	694.10	0.1791	557.36
ETTm ₁	24	0.6878	842.76	0.7036	1335.71	0.1777	542.67	0.1075	1029.65
	48	0.6994	899.90	0.7148	1546.38	0.1831	606.23	0.1162	317.65
	168	0.7765	1135.78	0.7582	2192.51	0.1853	695.64	0.1120	1102.62
	288	0.9372	2014.46	0.8598	2591.67	0.1805	954.43	0.1835	2690.85
	672	1.0269	3654.97	0.7848	3989.08	0.1799	1341.47	0.1960	2761.32
ECL	48	0.6518	555.99	0.7089	1010.28	0.2566	1459.48	0.1245	290.75
	168	0.8908	938.61	0.9080	1667.01	0.2482	1664.97	0.1205	696.57
	336	0.9236	1466.83	0.9468	2297.83	0.2696	1927.64	0.1377	1297.49
	720	1.1052	2608.97	0.8800	3592.86	0.3195	2566.90	0.2273	3352.05
	960	1.2642	4298.18	0.9097	4473.98	0.3396	2858.18	0.2463	3445.76

many of the datasets here. The experimental set-up is:

- Run simulations on the Informer model using full attention instead of probparse.
- Collect the full attention matrix of the first encoder block of the Informer.
- Given a window size w , compute the condition numbers of $w \times w$ sub-matrices along the diagonal of the attention matrix.
- If the condition numbers are finite, then BDI is true

and this instance is collected for a histogram plot, otherwise it is counted as a failure.

Using the procedure above, we plot all condition numbers for all simulations of the datasets in the paper. For all the simulations, we use the same hyper-parameters as in the experiment sections. Due to memory space constraint, we report the first 11 batches of the test datasets.

From Figs. 5, 6, 7, we observe that ETTh₁, Weather, ILI datasets satisfy the assumption of the theorem relatively well. In particular, ETTh₁ and ILI do not have many infinite condition numbers. The Weather dataset has about

3% infinite condition numbers. We also noted that the condition numbers increase with the window size.

I. FWin and Nonparametric Regression

The full self-attention function (Vaswani et al., 2017) can be conceptualized as an estimator in a non-parametric kernel regression problem in statistics (Nguyen et al., 2022). Let the key vectors serve as the training inputs and the value vectors as the training targets. The key-value pairs $\{k_j, v_j\}$ for $j = 1, \dots, N$, come from the model

$$v_j = f(k_j) + \epsilon_j, \quad (30)$$

where f is an unknown function to be estimated and ϵ_j are zero mean independent noisy perturbations. Let the key vectors k_1, k_2, \dots, k_N be i.i.d. samples from a distribution function $p(k)$, and the key-value pairs $(v_1, k_1), \dots, (v_N, k_N)$ be i.i.d. samples from the joint density $p(k, v)$. Since $\mathbb{E}[v_j | k_j] = f(k_j)$, the classical Nadaraya-Watson method (Nadaraya, 1964; Parzen, 1962; Rosenblatt, 1956) approximates p by a sum of Gaussian kernels and gives the estimate of f below:

$$\hat{f}_\sigma(k) := \sum_{j=1}^N \frac{v_j \phi_\sigma(k - k_j)}{\sum_{j=1}^N \phi_\sigma(k - k_j)}, \quad (31)$$

where $\phi_\sigma(\cdot)$ is the isotropic multivariate Gaussian density function with diagonal covariance matrix $\sigma^2 \mathbf{I}_D$. In particular if $k = q_i$, and the k_j 's are normalized, one obtains $\hat{f}_\sigma(q_i) =$

$$\frac{\sum_{j=1}^N v_j \exp(q_i k_j^T / \sigma^2)}{\sum_{j=1}^N \exp(q_i k_j^T / \sigma^2)} = \sum_{j=1}^N \text{softmax}(q_i k_j^T / \sigma^2) v_j. \quad (32)$$

Letting $\sigma^2 = \sqrt{d_{\text{model}}}$, where d_{model} is the dimension of q_i (k_j), turns estimator (32) into the softmax self-attention (1).

To build a window attention, we allow the query vector q_i to interact only with nearby key and value vectors. Thus the window version of the softmax estimator is $\bar{f}_\sigma(q_i) :=$

$$\frac{\sum_{j \in J(i)} v_j \exp(q_i k_j^T / \sigma^2)}{\sum_{j \in J(i)} \exp(q_i k_j^T / \sigma^2)} = \sum_{j \in J(i)} \text{softmax}(q_i k_j^T / \sigma^2) v_j$$

where $J(i)$ is the index set that correspond to the set of keys the query q_i interact with. In view of the fully connected (MLP) layer after the Fourier mixing layer and before the output in Fig. 1, we define the analogous FWin estimator for the regression model as

$$\tilde{f}_\sigma(q_i) := A \cdot \mathcal{R}(\mathcal{F}(\bar{f}_\sigma(q_i))), \quad (33)$$

where \mathcal{R} takes the real part, \mathcal{F} is the discrete Fourier transform, \cdot represents matrix multiplication, and A is a real matrix to be learned from the training data by minimizing the sum of squares error (MSE) of the regression model (30).

Kernel Regression Experiment To examine the differences among the three estimators \hat{f} , \bar{f} , and \tilde{f} , we opt for the Laplace distribution function $f = \exp(-\alpha|x|)$, for $\alpha = 0.01$, as the ground truth nonlinear function acting componentwise on the input to the regression model (30). We use a set of query, key, value vectors from Informer[†] (Zhou et al., 2021) on ETTh₁ multivariate data set with prediction length (metric) of 720. We choose this particular data set because Informer[†] (Zhou et al., 2021) with full softmax self-attention has the best performance there. The key vectors may not satisfy the theoretical i.i.d. assumption (Nguyen et al., 2022). In this experiment, we have a set of 168 query and key vectors from each of the 8 heads. Denote query q_i , and key k_j vectors for $i, j = 1, 2, \dots, 168$. The value vectors are $v_j = f(k_j)$. We divide the data into 136 vectors for training and the remaining 32 for testing. The mean square error (MSE) in testing of the estimator $\hat{f}(q_{i_n})$ for $n = 1, 2, \dots, 32$, are labeled full estimator in Fig. 8. Similarly, we compute MSEs for $\bar{f}_\sigma(q_{i_n})$, and $\tilde{f}(q_{i_n})$, using window size of 4, where A is learned by solving a least squares problem. Fig. 8 compares the MSE of the three estimators over data from 8 heads. We observe that the FWin estimator consistently outperforms the window attention estimator, and approaches the full softmax attention. In heads 0/1/4, FWin outperforms the full softmax attention estimator which is not theoretically optimal for the regression task (Nguyen et al., 2022). In conclusion, the regression experiment on the three estimators indicates that FWin is a simple and reliable local-global attention structure with competitive capability, lending added support to its robust performance.

Fourier-Mixed Window Attention

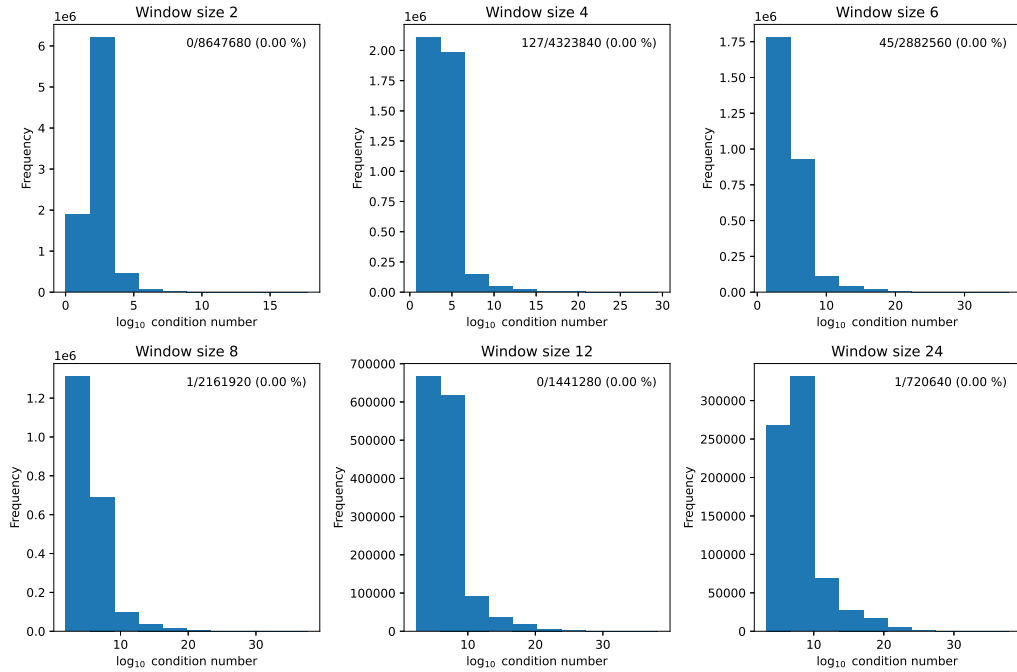


Figure 5. Condition number of ETTh1 (M) dataset under various window sizes. On the top right corner of each subplot there is a label “ n/m (k %)”, here m denotes the total number of condition numbers, n denotes the number of condition numbers that are infinite, and k denote the percentage of condition numbers that is infinite.

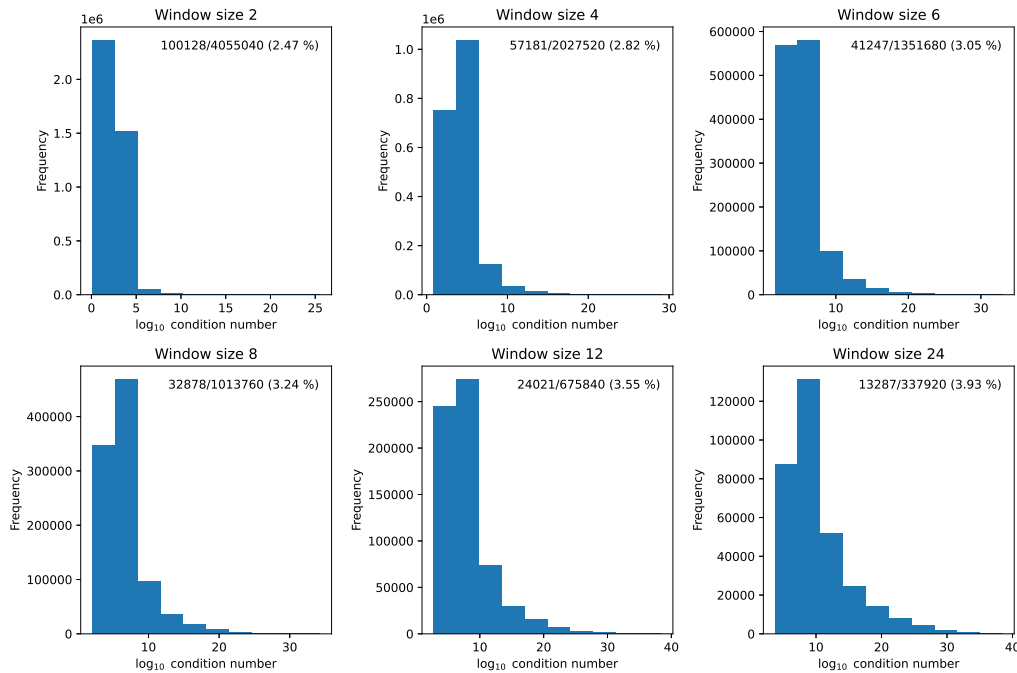


Figure 6. Condition number of Weather (M) dataset under various window sizes. On the top right corner of each subplot there is a label “ n/m (k %)”, here m denotes the total number of condition numbers, n denotes the number of condition numbers that are infinite, and k denote the percentage of condition numbers that is infinite.

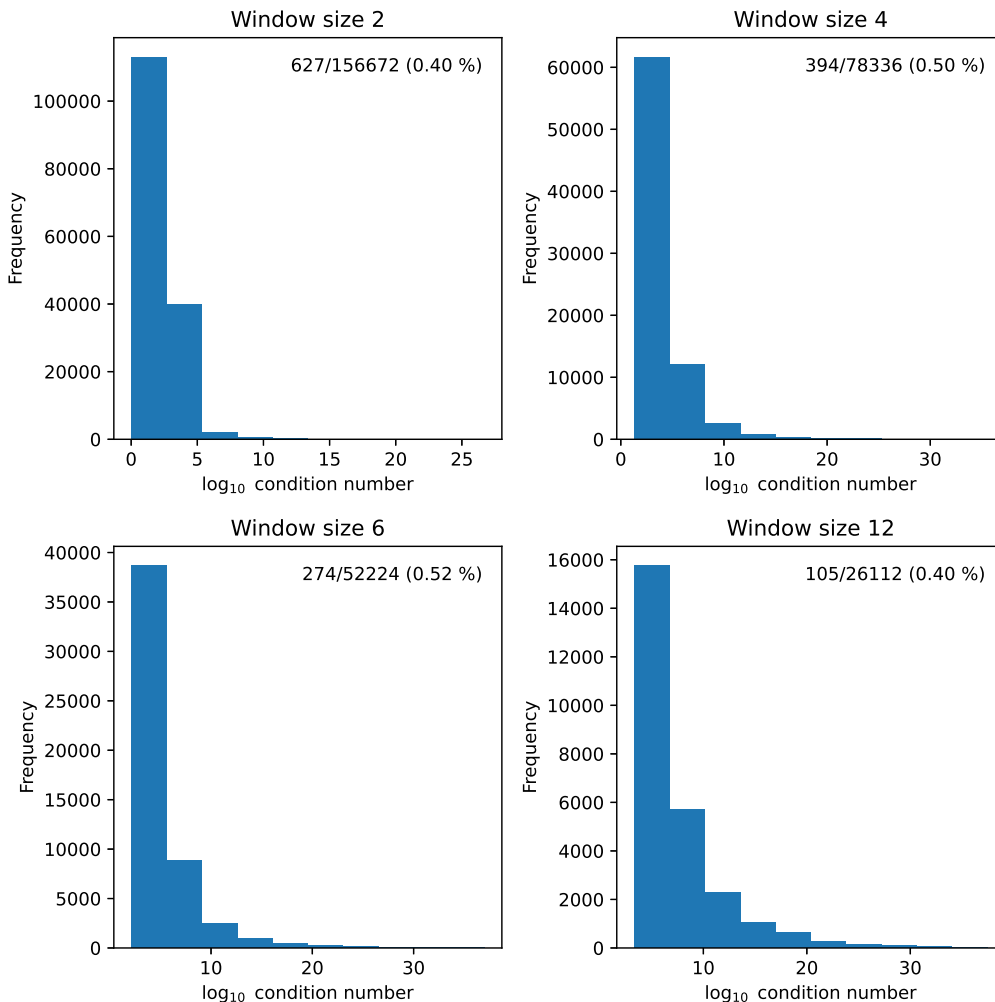


Figure 7. Condition number of ILI (M) dataset under various window sizes. On the top right corner of each subplot there is a label “n/m (k%)”, here m denotes the total number of condition numbers, n denotes the number of condition numbers that are infinite, and k denote the percentage of condition numbers that is infinite.

References

- Bracewell, R. N. *The Hartley Transform*. Oxford University Press, New York, 1986.
- Chow, J. and Rogers, G. Power system toolbox. Available at <https://www.ecse.rpi.edu/~chowj/>, 2008. Accessed: 2023-07-19.
- Guibas, J., Mardani, M., Li, Z., Tao, A., Anandkumar, A., and Catanzaro, B. Efficient token mixing for transformers via adaptive Fourier neural operators. *International Conference on Learning Representations*, 2022.
- Lai, G., Chang, W.-C., Yang, Y., and Liu, H. Modeling long- and short-term temporal patterns with deep neural networks, 2018.
- Lee-Thorp, J., Ainslie, J., Eckstein, I., and Ontanon, S. Fnet: Mixing tokens with Fourier transforms. *arXiv:2105.03824*, 2021.
- Li, J., Yue, M., Zhao, Y., and Lin, G. Machine-learning-based online transient analysis via iterative computation of generator dynamics. in *Proc. IEEE SmartGridComm*, 2020.
- Li, M., Zhao, X., Liu, R., Li, C., Wang, X., and Chang, X. Generalizable memory-driven transformer for multivariate long sequence time-series forecasting. *arXiv preprint arXiv:2207.07827*, 2022.
- Liu, Z., Lin, Y., Cao, Y., Hu, H., Wei, Y., Zhang, Z., Lin, S., and Guo, B. Swin transformer: Hierarchical vision transformer using shifted windows. *IEEE/CVF Confer-*

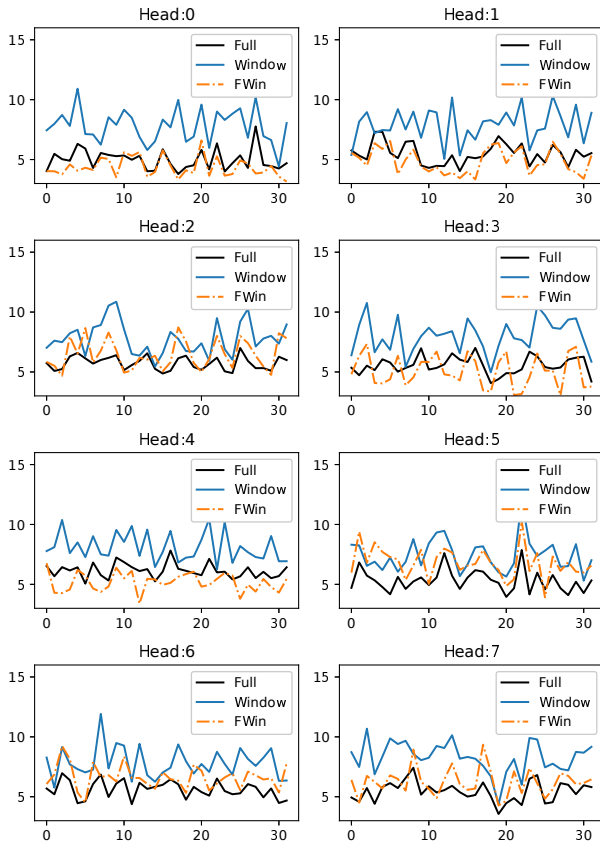


Figure 8. MSE error vs. query number comparison of full softmax attention (black), window attention (blue) and FWin attention (orange) in the non-parametric regression model (30) based on key vectors of a full attention layer of Informer[†] (Zhou et al., 2021) trained from the ETTh₁ data set.

ence on Computer Vision and Pattern Recognition, pp. 12009–12019, 2022.

Mehta, S. and Rastegari, M. Mobilevit: Light-weight, general-purpose, and mobile-friendly vision transformer. *ICLR*, 2022.

Nadaraya, E. On estimating regression. *Theory of Probability and its Applications*, 9:141–142, 1964.

Nguyen, T., Pham, M., Nguyen, T., Nguyen, K., Osher, S., and Ho, N. Fourierformer: Transformer meets generalized Fourier integral theorem. *Advances in Neural Information Processing Systems*, 2022.

Nie, Y., Nguyen, N. H., Sinthong, P., and Kalagnanam, J. A time series is worth 64 words: Long-term forecasting with transformers. In *The Eleventh International Conference on Learning Representations*, 2023. URL <https://openreview.net/forum?id=Jbdc0vTOcol>.

Parzen, E. On estimation of a probability density function and mode. *Annals of Mathematical Statistics*, 33:1065–1076, 1962.

Rao, Y., Zhao, W., Zhu, Z., Lu, J., and Zhou, J. Global filter networks for image classification. *Advances in Neural Information Processing Systems*, 34:980–993, 2021.

Rosenblatt, M. Remarks on some nonparametric estimates of a density function. *Annals of Mathematical Statistics*, pp. 832–837, 1956.

Tolstikhin, I., Houlsby, N., Kolesnikov, A., Beyer, L., Zhai, X., Unterthiner, T., Yung, J., Keysers, D., Uszkoreit, J., and Lucic, M. Mlp-mixer: An all-mlp architecture for vision. *arXiv preprint arXiv:2105.01601*, 2021.

Vaswani, A., Shazeer, N., Parmar, N., Uszkoreit, J., Jones, L., Gomez, A., Kaiser, L., and Polosukhin, I. Attention is all you need. *Advances in neural information processing systems*, 30, 2017.

Woo, G., Liu, C., Sahoo, D., Kumar, A., and Hoi, S. Etsformer: Exponential smoothing transformers for time-series forecasting, 2022.

Wu, H., Xu, J., Wang, J., and Long, M. Autoformer: Decomposition transformers with Auto-Correlation for long-term series forecasting. In *Advances in Neural Information Processing Systems*, 2021.

Yang, C., Qiao, S., Yu, Q., Yuan, X., Zhu, Y., Yuille, A., Adam, H., and Chen, L.-C. Moat: Alternating mobile convolution and attention brings strong vision models. *arXiv preprint arXiv:2210.01820*, 2022.

Zheng, Y., Hu, C., Lin, G., Yue, M., Wang, B., and Xin, J. Glassformer: a query-sparse transformer for post-fault power grid voltage prediction. *Proc. of IEEE International Conference on Acoustics, Speech, and Signal Processing*, pp. 3968–3972, 2022.

Zhou, H., Zhang, S., Peng, J., Zhang, S., Li, J., Xiong, H., and Zhang, W. Informer: Beyond efficient transformer for long sequence time-series forecasting. in *Proc. of the Association for the Advancement of Artificial Intelligence*, 35:11106–11115, 2021.

Zhou, H., Li, J., Zhang, S., Zhang, S., Yan, M., and Xiong, H. Expanding the prediction capacity in long sequence time-series forecasting. *Artificial Intelligence*, 318:103886, 2023. ISSN 0004-3702.

Zhou, T., Ma, Z., Wen, Q., Wang, X., Sun, L., and Jin, R. Fedformer: Frequency enhanced decomposed transformer for long-term series forecasting. *International Conference on Machine Learning*, 2022.